PNAS

Supplementary Information for

Molecular determinants of pH sensing in the proton-activated chloride channel

James Osei-Owusu[1], Ekaterina Kots[2], Zheng Ruan[3], Ljubica Mihaljević[1], Kevin Hong Chen[1], Ami Tamhaney[1], Xinyu Ye[3], Wei Lü[3], Harel Weinstein[2], Zhaozhu Qiu[1,4*]

Affiliations:

[1]Department of Physiology, Johns Hopkins University School of Medicine, Baltimore, MD, 21205, USA.

[2]Department of Physiology and Biophysics, Weill Cornell Medicine, New York, NY, 10065, USA.

[3]Department of Structural Biology, Van Andel Institute, Grand Rapids, MI, 49503, USA.

[4]Solomon H. Snyder Department of Neuroscience, Johns Hopkins University School of Medicine, Baltimore, MD, 21205, USA.

[*]Correspondence: zhaozhu@jhmi.edu

This PDF file includes:

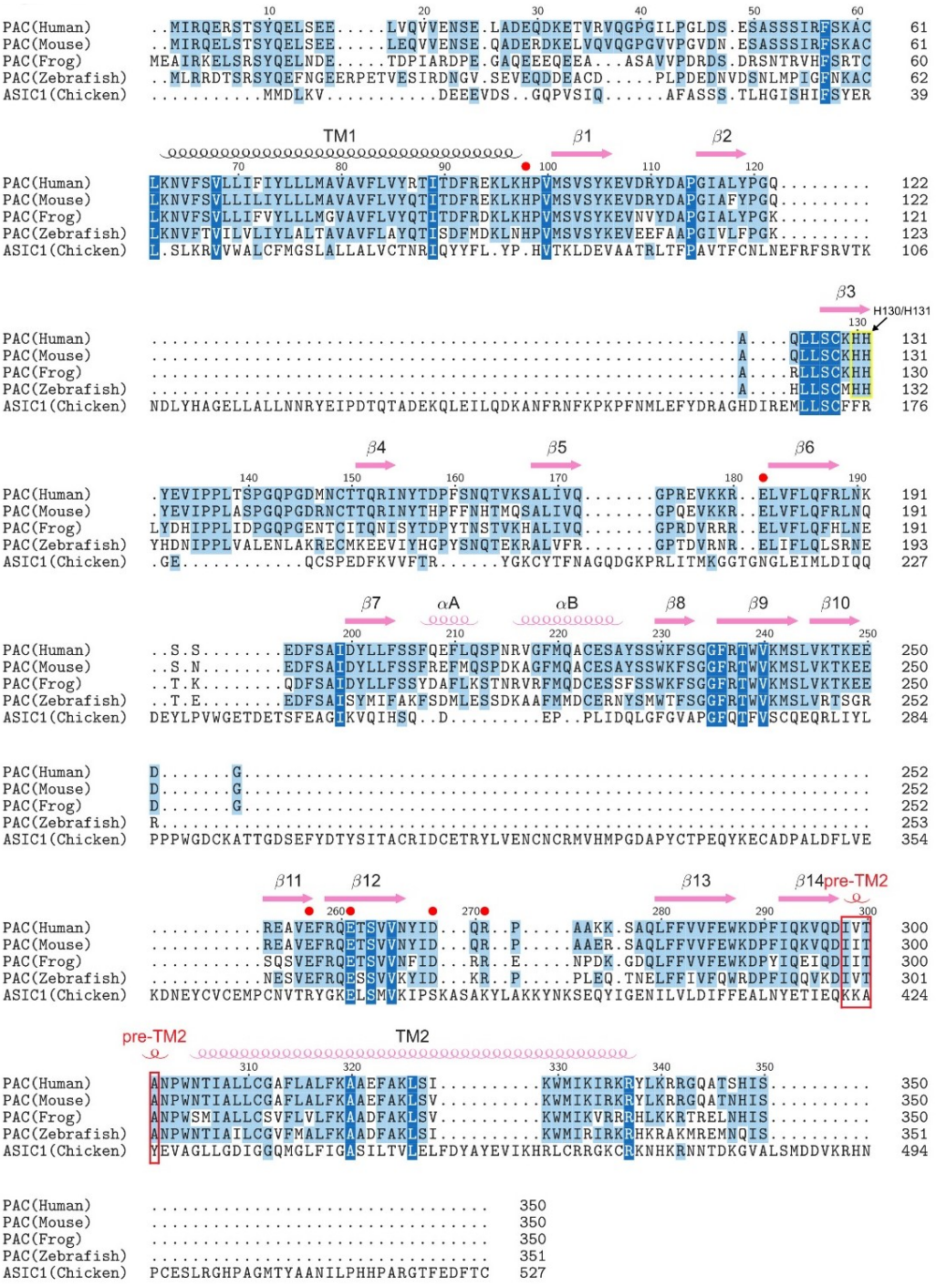

Figure S1. Sequence alignment of PAC homologues and ASIC. Sequence alignment of PAC homologues (from human, mouse, frog and zebrafish) and chicken ASIC1. The ASIC1 sequence is aligned with PAC based on the structural alignment using TMalign (1). Secondary structural (SS) elements of PAC are labeled at the top. Residues relevant to this study are marked with red dots. H130 and H131 are indicated with a yellow frame. The pre-TM2 helix observed in the pH4-PAC structure is indicated with a red frame.

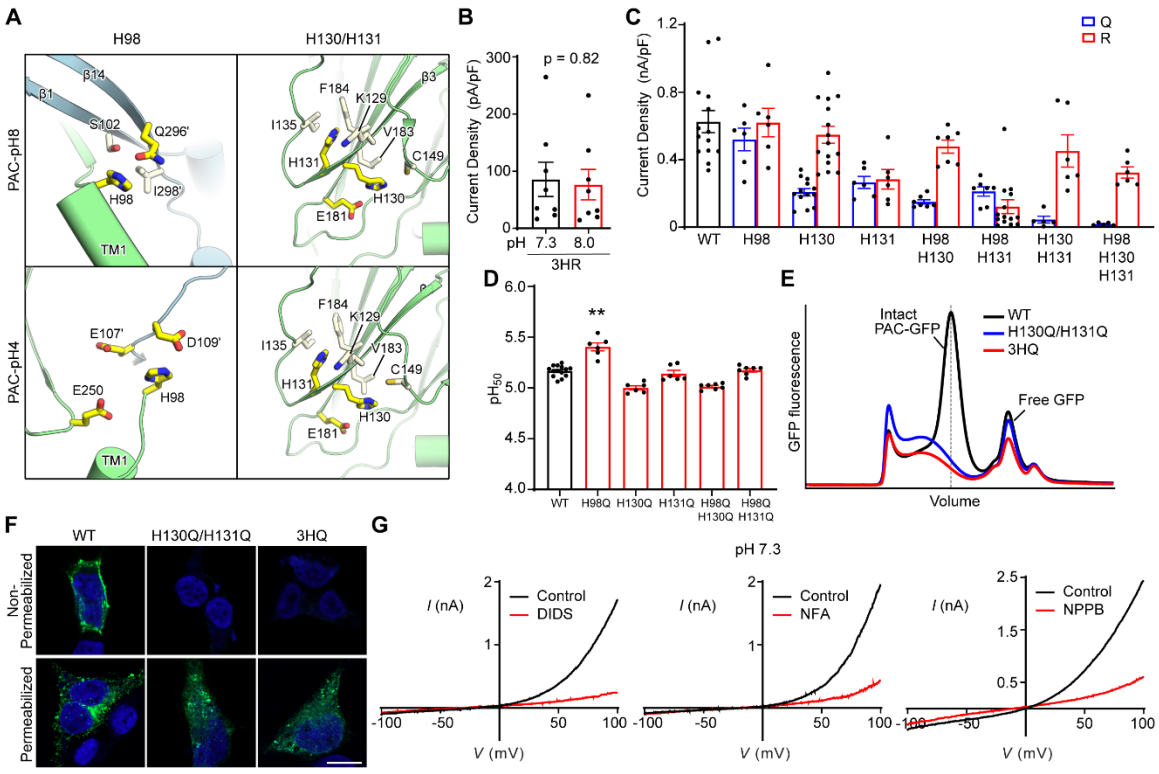

Figure S2. Characterization of PAC mutations of three histidine residues (H98, H130, and H131). (***A***) A close-up view of H98, H130 and H131 of PAC at both pH 8 and 4 (2). Residues from adjacent subunits are labeled with a prime symbol. **(*B*)** pH-8.0 and pH-7.3-induced current densities (mean ± SEM) of 3HR mutant at +100 mV. p = 0.82, two-tailed Student's *t* test. **(*C*)** pH-4.6-induced current densities (mean ± SEM) at +100 mV of wild-type PAC (the same values as in Fig. 1*C*), and glutamine (Q) and arginine (R) mutants of H98, H130 and H131. **(*D*)** pH_{50} values (mean ± SEM) of wild-type PAC (the same values as in Fig. 2*B*) and histidine mutants. The estimated pH_{50} was generated from the nonlinear fitting to a sigmoidal dose-response curve for each mutant. **p < 0.01, one-way ANOVA with Bonferroni post hoc test. **(*E*)** The FSEC profile of GFP-tagged wild-type PAC (black), H130Q/H131Q (blue) or H98Q/H130Q/H131Q (3HQ) (red) solubilized using GDN detergent. Expected position of intact GFP-tagged PAC protein is indicated in a dotted vertical line. **(*F*)** Cell surface immunostaining of HEK293T PAC KO transiently transfected with wild-type PAC-FLAG^{277} (the same representative image as Fig. 1*E*), H130Q/H131Q or 3HQ cDNA construct. Scale bar: 10 µm. **(*G*)** Examples of inhibition by the PAC channel blockers on 3HR-mediated basal currents at pH 7.3.

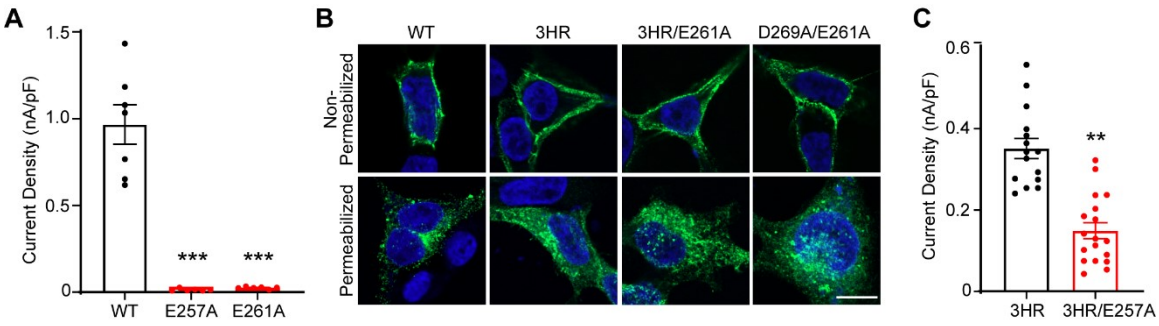

Figure S3. The joint region is important for PAC channel function. (*A*) Current densities of wild-type PAC, E257A and E261A mutants. Data are mean ± SEM of pH-4.0-induced currents at +100 mV. ***p < 0.001, one-way ANOVA with Bonferroni post hoc test. **(*B*)** Non-permeabilized and permeabilized HEK293T PAC KO cells expressing PAC-FLAG^{277} were immunostained with antibody against FLAG (wild-type is the same representative image as Fig. 1*E*). Scale bar: 10 µm. **(*C*)** Current densities of 3HR and 3HR/E257A. Data are mean ± SEM of pH-4.6-induced currents at +100 mV. **p < 0.01, two-tailed Student's *t* test.

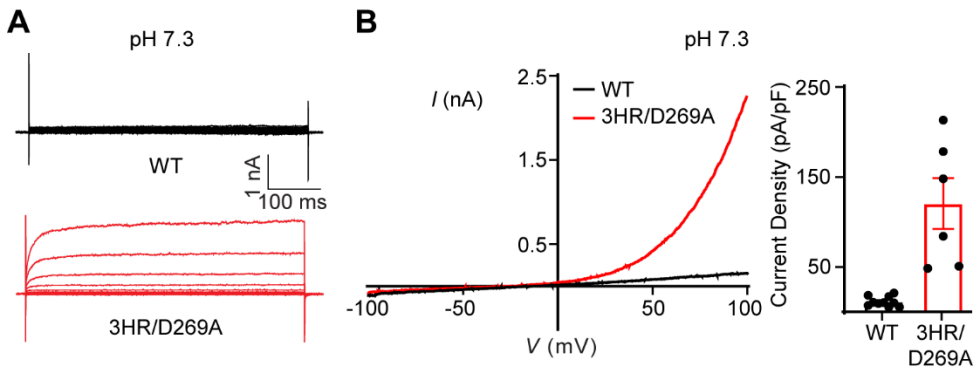

Figure S4. 3HR/D269A mutant mediates large basal currents at neutral pH. (*A*) Representative whole-cell currents of WT (top) and 3HR/D269A (bottom) mutant at pH 7.3 monitored by voltage-step protocol. **(*B*)** Left: representative whole-cell currents of wild-type PAC (black) and 3HR/D269A (red) at pH 7.3 monitored by voltage ramp protocol. Right: current densities (mean ± SEM) at +100 mV of wild-type PAC and 3HR/D269A at pH 7.3.

A

NbIT Site	Residue list
S1	R87, D91, R93, E94, K95
S2	K97, H98
S3	K246, K248, E249, E250, D251, R253, E254
S4	K106, E107, K294
S5	D109, R110, D112
S6	R175, E176, K178, K179, R180, E181
S7	K129, H130, H131, E133
S8	K288, D289
S9	E257, R259, E261
S10	K319, E322, K325
S11	D200, K231
S12	K191, E194, D195
S13	K275, K276
S14	K241, E286
S15	D269, R271
S16	R56, K59, K63

B

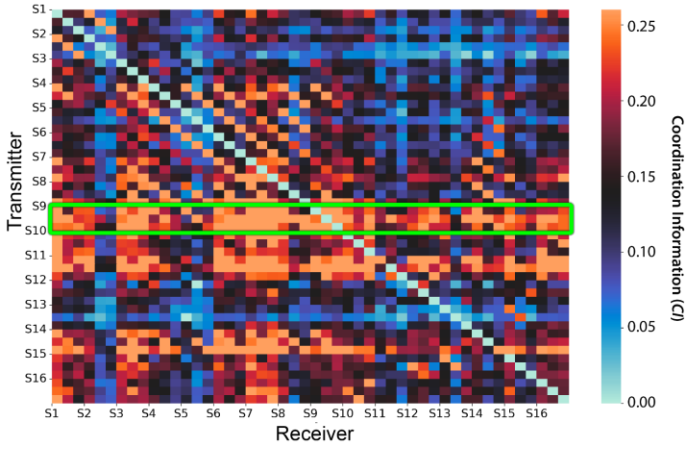

Figure S5. Parameters for the preliminary stage of NbIT analysis of PAC MD simulations. (*A*) Per-subunit list of NbIT sites of the initial analysis. **(*B*)** 2D-heatmap of Coordination Information (*CI*) shared between PAC titratable sites as defined on the first stage of NbIT analysis (*A*) at pH 4. Each NbIT site is represented by three map points. S9 site is highlighted with a green frame.

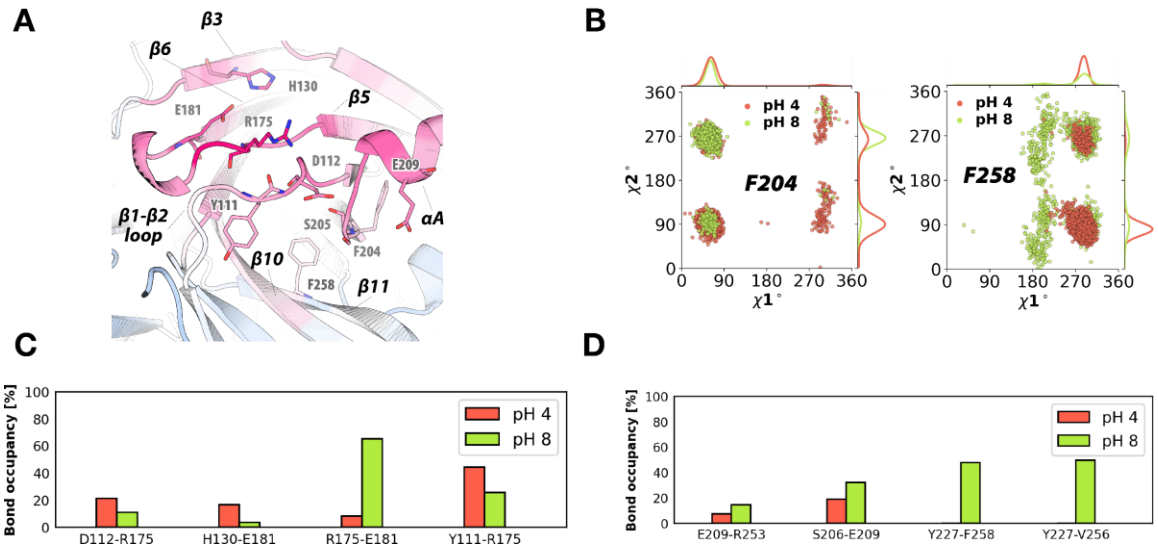

Figure S6. Specific interactions associated with the pH-dependence of allosteric signaling between the H130 region and TM1 in the ECpH MD simulations trajectories obtained for the PAC trimer at pH 4 and pH 8. (*A*) Structure detail of the "transmitter" region of allosteric pathway (H130 region). **(*B*)** Distribution of sidechain dihedrals of F204 and F258 at pH 4 and pH 8. **(*C-D*)** Occupancies of specific non-bonded interactions along the H130/H131-to-TM1 allosteric pathway, at pH 4 and pH 8.

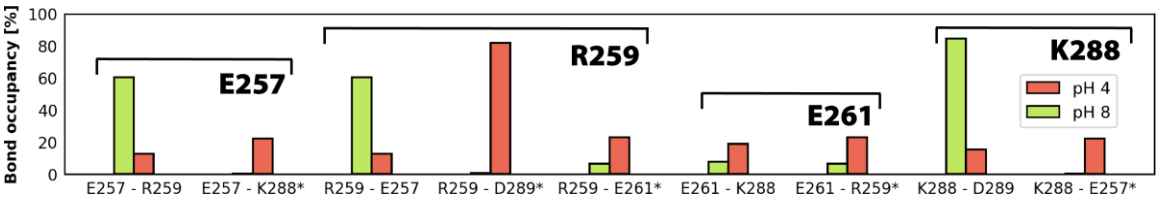

Figure S7. Occupancies of pH-dependent inter-subunit interactions in the ECpH MD simulation trajectories. The occupancies of salt-bridge non-bonded interactions in the joint region of the protein evaluated from ECpH MD simulations of wild-type PAC protein at pH 4 (coral) and 8 (lime green). The cutoff radius was set to 4 Å. Asterix indicates residues from a neighboring subunit.

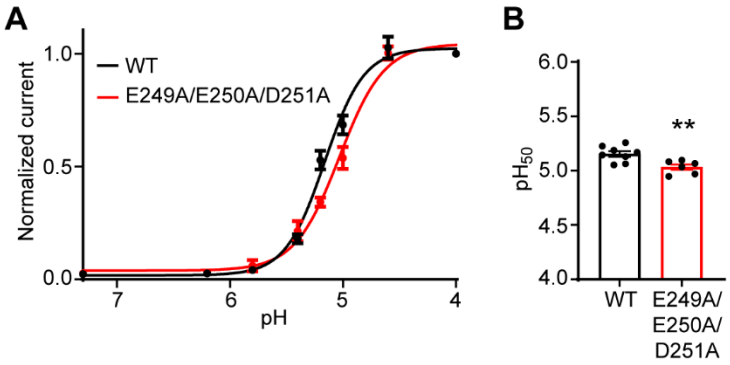

Figure S8. 3HR/D269A mutant mediates large basal currents at neutral pH.
(*A*) pH dose-response curve of wild-type PAC (black) and E249A/E250A/D251A (red). The currents are normalized to the pH-4.0-induced currents (n = 8 (wild-type PAC); n = 6 (E249A/E250A/D251A)). The normalized data are fitted to Hill equation unconstrained, allowing both the top and bottom to be defined by the maximum and minimum normalized currents. Data are mean ± SEM of the normalized currents at +100 mV. **(*B*)** pH_{50} values (mean ± SEM) of wild-type PAC and E249A/E250A/D251A mutant estimated from the pH dose-response curve in (*A*). **p < 0.01, two-tailed Student's *t* test.

Table S1. Root Mean Square Fluctuation (RMSF) values calculated for the Cα atoms of the β-strands in PAC from equilibrated segments of MD trajectories at pH 4 and 8.

		RMSF [Å]		
		pH 4	pH 8	% Increase
β1	M101 – E107	1.6	2.3	+44%
β2	P114 – P120	1.3	1.8	+38%
β3	Q124 – Y132	1.7	2.1	+24%
β4	T150 – T157	2.1	2.8	+33%
β5	V162 – Q172	2.5	3.0	+20%
β6	E181 – N190	1.5	1.8	+20%
β7	S197 – F204	1.2	1.8	+33%
β8	S229 – S233	1.1	1.6	+45%
β9	G235 – K243	1.1	1.6	+45%
β10	V245 – E250	2.2	2.7	+23%
β11	E253 – E257	1.9	2.4	+26%
β12	R259 – N266	1.1	1.5	+36%
β13	N279 – W287	1.2	1.5	+25%
β14	P290 – D297	1.5	2.1	+40%

SI References

1. Y. Zhang, J. Skolnick, TM-align: a protein structure alignment algorithm based on the TM-score. *Nucleic Acids Res* **33**, 2302-2309 (2005).

2. Z. Ruan, J. Osei-Owusu, J. Du, Z. Qiu, W. Lü, Structures and pH-sensing mechanism of the proton-activated chloride channel. *Nature* (2020).